ISSN 8756-6990, Optoelectronics, Instrumentation and Data Processing, 2023, Vol. 59, No. 6, pp. 693–702. © Allerton Press, Inc., 2023.
Russian Text © The Author(s), 2023, published in Avtometriya, 2023, Vol. 59, No. 6, pp. 41–51.

OPTICAL-PHYSICAL METHODS OF RESEARCH AND MEASUREMENT

Determination of the Pore Direction in a Crystalline Metal-Organic Framework by Raman Spectroscopy and Periodic Calculations Based on the Electron Density Functional Theory

N. V. Slyusarenko[1], I. D. Yushina[2], E. A. Slyusareva[1], E. V. Golovkina[3], S. N. Krylova[3], A. N. Vtyurin[3], and A. S. Krylov[#3*]

[1] *Siberian Federal University, Krasnoyarsk, 660041 Russia*

[2] *South Ural State University, Chelyabinsk, 454080 Russia*

[3] *Kirensky Institute of Physics, Siberian Branch, Russian Academy of Sciences, Krasnoyarsk, 660036 Russia*

Received July 15, 2023; revised August 1, 2023; accepted August 2, 2023

Abstract—A method for the determination of pore orientation in metal-organic framework structures by polarized Raman spectra is proposed. The method involves sensitivity of the line intensity of Raman scattering to the geometry of propagation in a crystal. The operability of the method is shown by DUT-8 (Ni, Co) crystals. The obtained results are interpreted based on analysis of symmetry and direction of vibrations within periodic calculations of the electron density functional theory. The simultaneous approach allowed us to describe the vibrations and to find the principal crystal orientation collinear to the pore direction. The information on the pore orientation is necessary for problems of adsorption and design of complex multicomponent materials based on metal-organic framework.

DOI: 10.3103/S8756699023060134

Keywords: *Raman light scattering, metal-organic framework, pore orientation, electron density functional theory*

INTRODUCTION

Polarized measurements are widely used to study anisotropic substances, especially for two-dimensional materials [1–3]. In addition, polarized Raman spectroscopy can reveal the crystallographic orientation [4], the orientation distribution of molecules [5, 6], and the azimuthal angle of materials in three dimensions [2]. Considerable success has already been achieved for layers of MoS_2 [7], WTe_2 [4], graphene [8], and insulated nanotubes [9]. Many present-day functional materials, such as optical crystals [10] and metal-organic frameworks (MOFs) [11], are also anisotropic; therefore, their physical properties sometimes significantly depend on orientation of a specific crystal. In some cases, orientation of crystals can be determined based on X-ray diffraction. However, for small crystal sizes (less than 0.1 mm), such measurements can be carried out only using strong synchrotron sources, which is often necessary for studying metal-organic frameworks.

Metal-organic frameworks are a promising class of hybrid materials with an ordered structure consisting of ions/clusters of metals and organic linkers [12]. Due to their porous structure, this class of composites is used for gas adsorption [13] and separation [14], catalysis [15], energy storage [16], drug delivery systems [17], and other applications. Some MOFs [18–20] are characterized by structural transitions related to the change in porosity as a response to external influences. One of such flexible metal-organic frameworks is the DUT-8 (Ni) (DUT, Dresden University of Technology; $Ni_2(ndc)_2(dabco)$, ndc

*E-mail: shusy@iph.krasn.ru
#Corresponding author.

is 2,6-naphthalenedicarboxylate and dabco 1,4-diazabicyclo[2.2.2]octane) [21]. The study of Raman light scattering spectra on this MOF shows a significant difference in the low-frequency region for open and closed DUT-8 (Ni) phases [22]. The transition from the phase with closed pores to the phase with open pores in DUT-8 (Ni) is influenced by the size and morphology [23], temperature [24], gas penetration [25, 26], and increase in hydrostatic pressure [27]. For DUT-8 (Ni), Ni ions were also partially replaced by Co ions [28].

However, some applications require correct orientation of crystallites to make the pore channel accessible for gas molecules. The small size of crystals and low intensity of diffraction require carrying out synchrotron investigations for such measurements of crystal morphology and correct orientation. Nevertheless, carrying out experiments of Raman spectroscopy can partially solve this problem at very small sizes of crystals with different orientation of incident and scattered light polarization, as well as in combination with rotation of the crystal. The abovementioned procedure in combination with calculation of active modes of Raman scattering based on the electron density functional theory (DFT) and corresponding interpretation can reveal the pore direction in different crystals. In this work, we demonstrate results of this approach for DUT-8 (Ni, Co) crystals in the open and closed phases. The feature of this work is related to the possibility of the open/closed pore phase transition in the DUT-8 (Ni, Co) framework; here, for this reason, results of this approach in both phases of DUT-8 (Ni, Co) crystals are demonstrated.

EXPERIMENT

The synthesis, crystalline structure, and chemical characteristic of DUT-8 (Ni, Co) crystals can be found in [26].

The Raman spectra were obtained in the geometry of backscattering on an Horiba Jobin-Yvon T64000 triple spectrometer (Horiba, France) operating the dispersion subtraction mode. A Spectra-Physics Excelsior-532–300 532 nm diode-pumped visible CW solid-state single-mode laser (United States) with a power of 5 mW at the sample was used as a spectrum excitation source. The incident laser beam was focused on the sample through an Olympus MPlan 50 lens with a numerical aperture N.A. = 0.75 and working distance of 1 mm. The same lens collected the scattered light.

The geometrical configuration of the experiment for a MOF sample with a random crystal plane is shown in Fig. 1.

The hypothetical crystalline packing fragments oriented along the long morphological axis of the needle-like crystal are shown to the left for the closed phase and to the right for the open phase.

Two series of experiments were carried out with parallel and cross-parallel polarizations of incident and scattered radiations for studying the angular dependence of Raman spectra line intensities. The shift of the incidence point of the exciting radiation was always within a circle with a diameter of 3 μm at the complete revolution through 2π. The complete revolution includes 60 measurement points with a step of $\pi/30$.

The experiment involved a single-crystal sample oriented along the long axis of a needle-shaped crystal with linear dimensions of about 70–100 μm. The direction of crystallographic axes for the given crystal is unknown. Analysis in a laboratory coordinate system different from the crystallographic system in rotations by Euler angles allows one to perform the following transformations.

The relative intensity of Raman modes can be represented as

$$I \sim (e_i R e_s)^2,$$

where I is the Raman scattering intensity; R is the Raman tensor; and e_i and e_s are the polarized unit vectors of incident and scattered light [29–31].

The parallel configurations e_i and e_s in Cartesian coordinates can be defined as $e_i = (0, 1, 0)$ and $e_s = (0, 1, 0)$; e_s in the cross-configuration in Cartesian coordinates can be found as $e_s = (1, 0, 0)$.

With allowance for the Euler matrix Φ_{xyz} and its inverse matrix $\Phi_{R_{xyz}}$ which transforms the crystal coordinates into experimental coordinates, the Raman scattering tensor is defined by the expression

$$R_{xyz} = \Phi_{xyz} R \Phi_{R_{xyz}}.$$

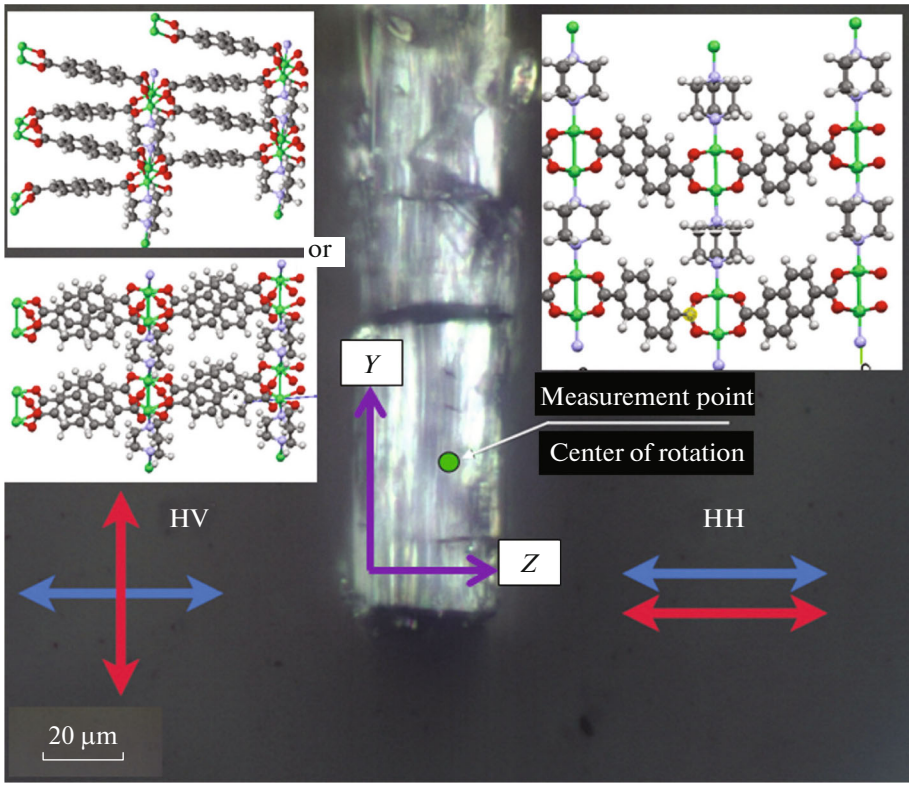

Fig. 1. Photograph of the crystal under study. Polarization of the exciting laser beam is marked by the blue arrow. Polarization of the scattered light is marked by the red arrow. The green point is the measurement point and the center of rotation. The fragment of the crystalline structure in the right upper part of the figure corresponds to the phase with open pores; in the left upper part, to the phase with closed pores at the initial measurement point at vertical orientation of the needle-like crystal. The crystalline structures of an unsubstituted DUT-8 (Ni) sample were taken as an example because these structures were considered for quantum-chemical modeling.

CALCULATION

The numerical calculations under the periodic boundary conditions were carried out by the CRYSTAL17 software [32]. Crystalline structures of unsubstituted DUT-8 (Ni) with open and closed pores were considered. It was necessary to neglect the influence of Co atoms, because the spectra of both substances exhibit a similar position of bands [26].

Atom positions (DFT/B3LYP) with fixed parameters of the cell were optimized using the 6-311G basis set for C, H, N, and O atoms and the TZVP set for Ni atoms. The K-point was sampled using the $4 \times 4 \times 4$ Monkhorst–Pack grid. The truncation criteria for bielectron integrals were established as follows: the overlap threshold for Coulomb integrals and Hartree–Fock exchange integrals is equal to 10^{-8} a.u., the penetration threshold for Coulomb integrals is equal to 10^{-8} a.u., and the first and the second pseudooverlap criteria are equal to 10^{-8} and 10^{-16} a.u., respectively; to increase the calculation quality, these values are higher than the default values. Positions of Raman active modes were calculated according to the Kohn–Sham methodology with pairwise perturbations. Negative modes were not observed in the Hesse matrix in the form with closed pores; for the form with open pores, two negative modes (-23 and -8 cm^{-1}) were obtained due to the initial disorder in the experimental crystalline structure in the absence of a solvent in the molecule pores. Due to the disorder in the structure with open pores, the crystal symmetry was reduced to the P1 space group, which led to 132 independent atoms in the elementary cell. Polarized Raman data were obtained for the xx, xy, xz, yy, yz, and zz directions for both phases. In these directions, the polarizability tensor and the intensity of modes were analyzed. The method for determining orientation of metal-organic framework pores is based on [4]. All lines of polarized Raman spectra measured in HH and HV geometries were analyzed in a similar way and fitted by the Lorenz function; the angular dependences of the line intensities were plotted in a polar coordinate system. Complicated lines were also decomposed into components using

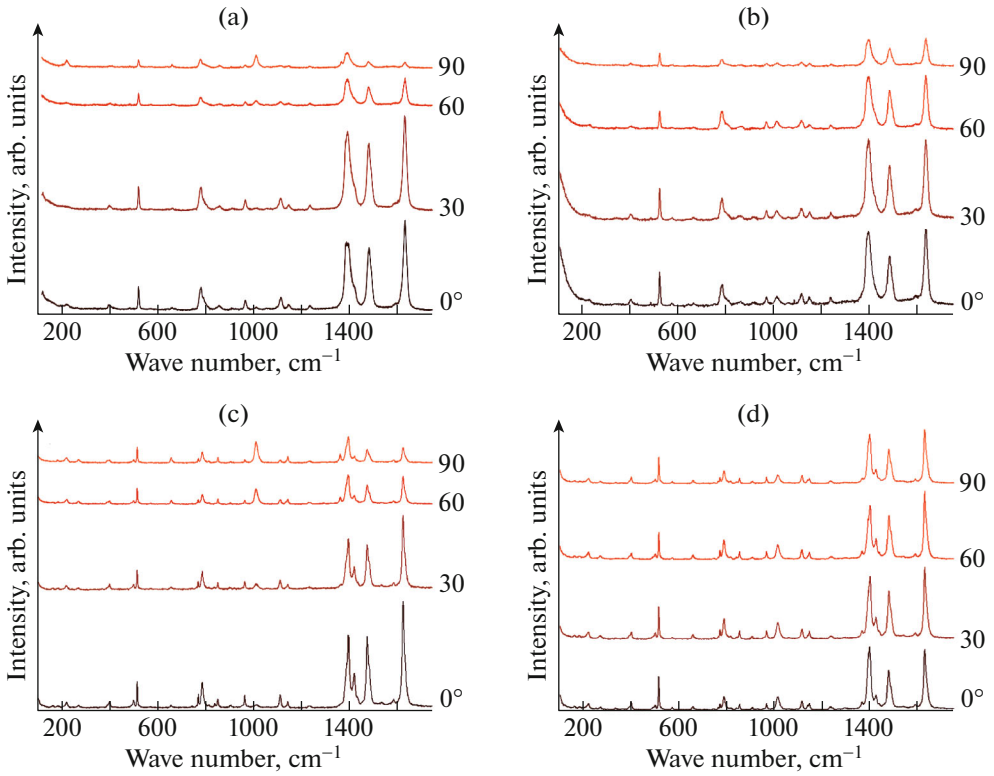

Fig. 2. Polarized Raman spectra for DUT-8 (Ni, Co): in the phase with (a, b) open and (c, d) closed pores for (a, c) parallel (HH) polarization of incident and scattered light relative to the crystal orientation and (b, d) cross (HV) polarization.

the Lorenz function. Based on the obtained angular dependences of the intensities, lines for which polar diagrams have the shape of two-petal diagrams were determined. Further, pairs of lines with opposite orientation of two-petal diagrams were chosen and the ratios of line intensities were found depending on macrocrystal rotation. By the relationship of intensities of the corresponding lines, it was possible to estimate the crystallographic orientation of the macrocrystal.

RESULTS AND DISCUSSION

Figure 2 presents selected results of polarization spectra of Raman scattering for DUT-8 (Ni) with 25% substitution by Co ions.

Two different polarizations are taken into account: parallel and cross polarization, as well as two phases with open and closed pores. Such variety of data made it possible to reveal several observations that become visible only when passing to polarized spectra. On the one hand, a clear antiphase behavior of bands corresponding to linkers‘ and dabco vibrations oriented orthogonally to each other in the crystalline structure of the phase with open pores is observed only in polarized Raman spectra of oriented crystals. On the other hand, it is well seen that partial substitution of nickel atoms by cobalt for most lines does not lead to a reliably detected change in the position of lines (the analysis is based on the previously performed detailed characteristic of spectra of pure DUT-8 (Ni) under different conditions [22, 27]).

Previously, it was shown that theoretical spectra well agree with nonpolarized Raman data [27]; in this work, however, this analysis is applied to polarized data for oriented crystals in an attempt to establish a direct correspondence for trends of changes in the intensity with respect to different directions inside the experimental and modeled crystals (Fig. 3).

For phases both in the experiment and in the calculations, the intensity of bands and modes in the cross-polarized mode is lower than in the corresponding parallel mode. The most significant difference

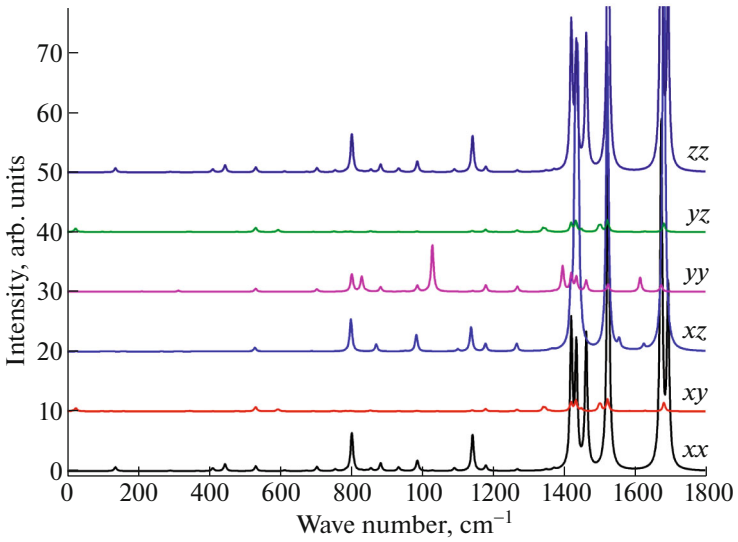

Fig. 3. Calculated Raman spectra of the DUT-8 (Ni) compound with open pores in the xx, xy, xz, yy, yz, and zz directions.

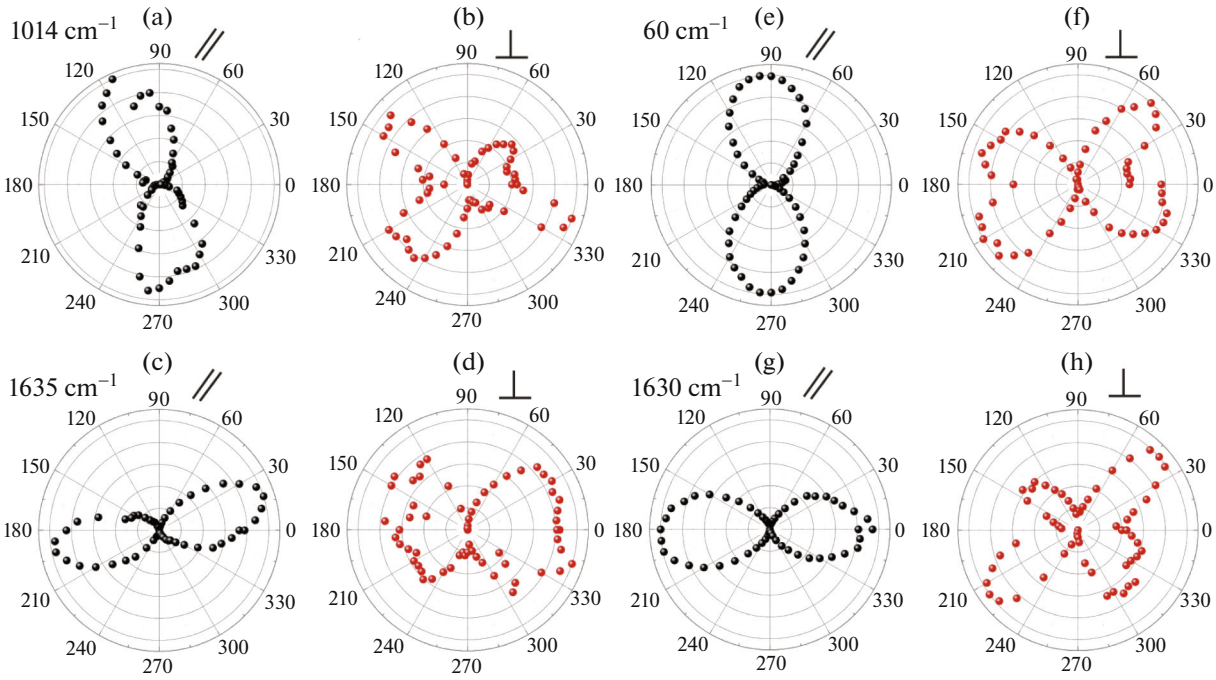

Fig. 4. Angular dependences of line intensities with respect to crystal rotation for the phase with open pores: lines of (a, b) 1014 and (c, d) 1635 cm^{-1} for (a, c) parallel and (b, d) cross polarization in a polar coordinate system.

in intensities of bands and modes of different directions is observed for the phase with open pores, which is related to features of its crystalline structure.

Let us analyze the angular dependences of polarized Raman spectra of the phase with open pores in a polar coordinate system. In total, several lines were approximated for this stage. In parallel polarization, only one line of 1014 cm^{-1} exhibits a typical vertical intensity distribution (Fig. 4a). The horizontal orientation of the petal diagrams was observed for the lines at 1115, 1485, and 1635 cm^{-1}. All other analyzed lines had the four-petal or even a more complicated shape. Cross (HV) polarization led to an almost four-petal shape for all lines, as it is shown in Figs. 4b and 4d for lines at 1014 and 1635 cm^{-1}.

According to theoretical calculations and interpretation presented in [27], the modes at 1014, 1115,

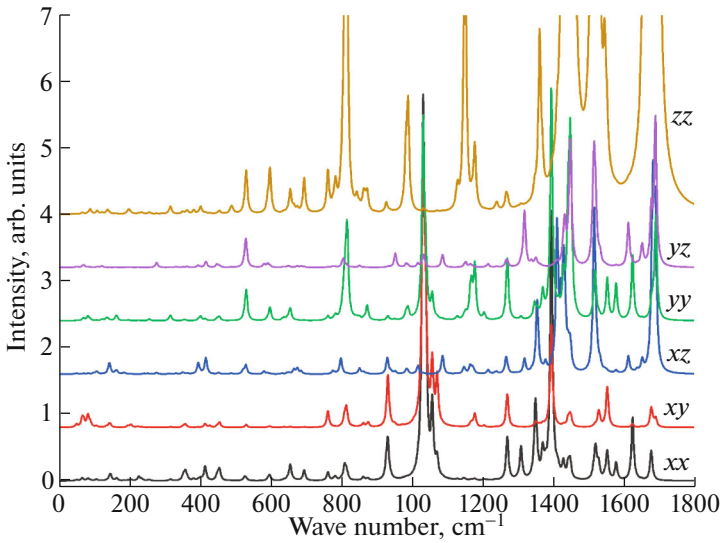

Fig. 5. Calculated Raman spectra of the DUT-8 (Ni) compound with closed pores in the xx, xy, xz, yy, yz, and zz directions.

1485, and 1635 cm^{-1} are related to C–C valence vibrations in the dabco fragment, Δ C–H oscillations in aromatic linkers, C–C valence vibrations in linkers, and elongation of the C=O bond in the carboxyl group of linkers, respectively. It is well seen that the spectra yy and zz orientations (and in the xx direction equivalent to it) well separate increments of dabco bands (the yy direction) and bands corresponding to vibrations of aromatic linkers (the zz direction) located orthogonally to each other according to the crystallographic scheme and theoretical data (see Fig. 1). Thus, the horizontal and vertical shapes of two-petal curves in experimental data in a polar coordinate system and theoretical Raman spectra in specific directions completely agree with each other. Such orthogonality in the crystal structure and the associated clear separation of increments belonging to different structural units makes it possible to use the ratiometric signal for conditions of crystal orientation relative to the pores direction inside it. Similarly to the phase with open pores, angular dependences of data on line intensities were analyzed for the phase with closed pores (Fig. 5).

We examined 21 spectral lines. All of them were intense and easily approximated by the Lorenz curve. The diagrams in polar coordinates for parallel polarization have the two- or four-petal shape. However, only the 60, 660, and 1014 cm^{-1} lines exhibit the vertical orientation of the intensity distribution (see Fig. 5 for the line of 60 cm^{-1}), and 13 lines at 401, 503, 518, 774, 791, 968, 1116, 1392, 1401, 1426, 1480, 1489, and 1630 cm^{-1} exhibit the horizontal orientation, as it is shown in Fig. 5 for the line at 1630 cm^{-1}. Other analyzed lines were characterized by the four-petal shape. Cross (HV) polarization usually led to the four-petal shape of the curve; in some case, no strict dependence of line intensities on the crystal orientation was observed.

According to the calculated polarized Raman scattering spectra, the antiphase behavior of the intensity of bands belonging to vibrations of aromatic linkers and fragments of dabco is observed even in spite of the fact that the characteristic motive of the quadratic grid for the phase with open pores does not exists anymore in the phase with closed pores. The most intense direction for vibration bands of linkers is zz, while the xx and yy directions are almost similarly intense for dabco valence vibrations observed at 1030 cm^{-1} in the calculated spectra. It should be noted that the relation of corresponding intensities of linkers to dabco oscillations in the phase with open pores is less noticeable than in the case of the phase with closed pores, where vibrations of linkers become even more intense in the zz direction due to orthogonality.

The interpretation of the results becomes more complicated when we examine the region of small wavenumbers. As was mentioned in [27], it is difficult to attribute the exact calculated mode to the most typical experimental band of 60 cm^{-1} because there exist many calculated modes in the region below 100 cm^{-1} (51, 68, 82, and 89 cm^{-1}) but no unambiguous definition was presented. However, when

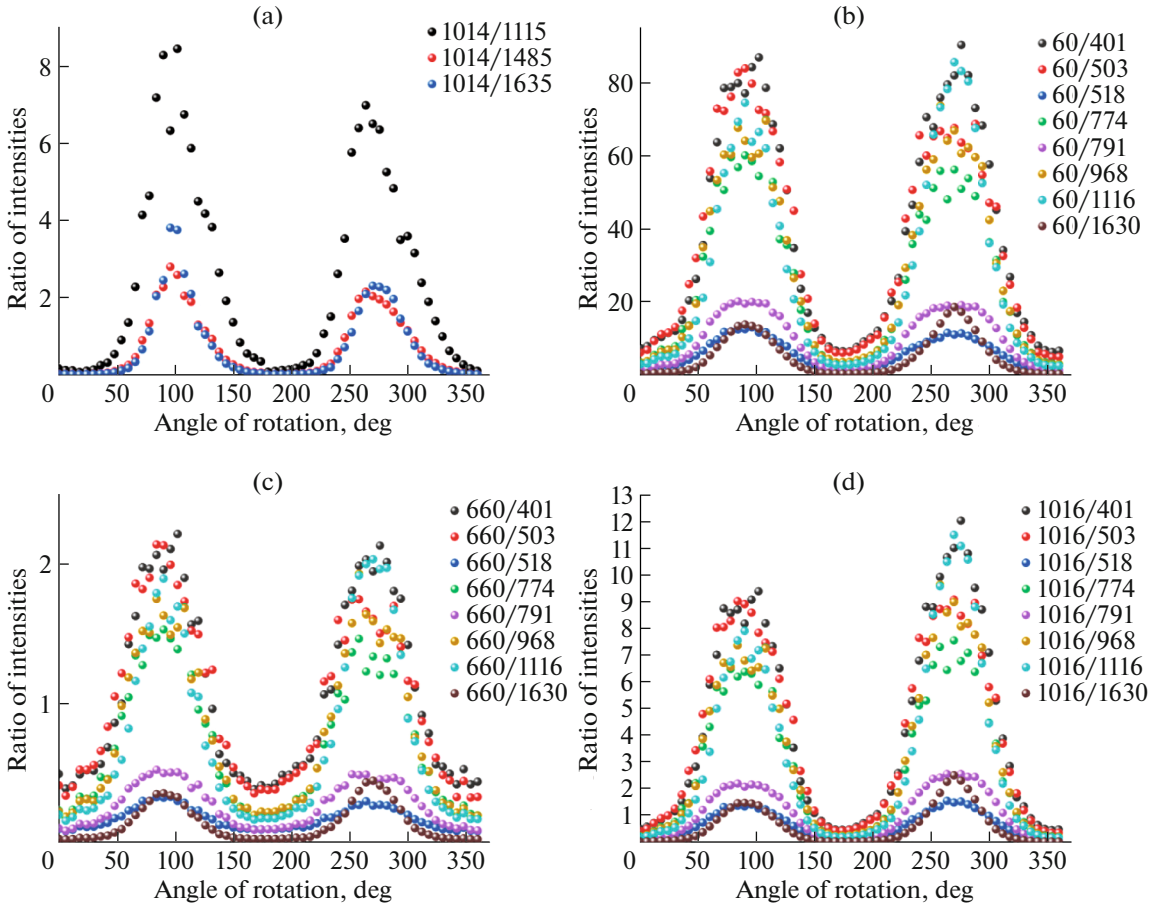

Fig. 6. Ratiometric signal calculated as the ratio of line intensities: in the phase (a) with open pores and (b, c, d) with closed pores.

we consider polarized experimental data, it becomes clear that the experimental band at 60 cm^{-1} has the same two-petal shape and orientation as the band at 1014 cm^{-1} due to dabco stretching. Thus, base on Fig. 4e, we can assume that the required calculated mode with which the experimental band at 60 cm^{-1} could be directly associated is rather the band at 51 cm^{-1} because this is the only mode that exhibits the clear antiphase behavior with bands in the zz (see Fig. 3, the blue curve). Therefore, using polarized spectra can not only solve problems of crystal orientation relative to the pore direction but also significantly approximate problems of band attribution in complex cases by multiple calculated data.

The revealed differences in polar diagrams for different types of lines formed the basis of the ratiometric relations for the phase with open pores (Fig. 6a) and the phase with closed pores (Figs. 6b–6d). For these purposes, the ratios of intensities of lines from the first group to the line intensity from the second group were calculated. Since the intensity of the 660 cm^{-1} line in the phase of closed pores is rather low, using the 60 and 1016 cm^{-1} lines is a preferable choice. The selection of lines from the second group should be limited by lines that do not require decomposition of complicated curves because this introduces possible additional errors into line amplitudes. Thus, among 13 analyzed lines, one may distinguish 8 lines: 401, 503, 518, 774, 791, 968, 1116, and 1630 cm^{-1}.

The line at about 1014 cm^{-1} can be used as a representative of the first group of lines attributed to dabco vibrations (the reference) both for the closed and for the open form of pores because the position of this line remains almost unchanged; it has high intensity and does not depend on the environment of the crystal. As a comparison line for the ratiometric signal, one may choose the 1115–1116 and 1630–1635 cm^{-1} lines which are attributed to vibrations of the Δ C–H and C=O bonds, respectively, according to theoretical calculations. These bands are also almost identical in phases with open and closed pores and do not require additional decomposition of complicated profiles in the analysis of

intensity. Such approach led to the determination of the crystal position up to $\pi/2$ in the phase with closed pores by data of the analysis of spectral line intensity in polarized Raman spectra in parallel polarization. Additional investigations in the phase with open pores made it possible to finally determine the pore direction. According to the studies, pores in DUT-8 (Ni, Co) in our experiment are directed along the Y axis (see Fig. 1). The pore direction for the open phase, in connection with the equivalence of two of three directions in the crystal, was quite unambiguously identified; at the same time, for the closed phase, due to structural closeness of motives in different directions and nonequivalence of all three directions in the crystal, establishing the pore direction unambiguously seems to be impossible and Fig. 1 presents two alternative orientations.

CONCLUSIONS

Based on polarized spectroscopic measurements of Raman scattering of oriented crystals, it has been shown that the pore direction inside a crystal can be determined in the general case owing to orthogonality of the motif. The specific antiphase behavior of 1015 cm^{-1} (dabco vibrations) and 1630–1635 cm^{-1} (vibrations of linkers) bands has been considered; the behavior remains stable regardless of the phase with open or closed pores, which made it possible to choose a line series suitable for constructing the ratiometric model of the signal. Thus, the pore direction was determined.

A detailed comparison of experimental and theoretical data in the region of small wavenumbers, allowed us to assign the line at 51 cm^{-1} to the mode corresponding to the experimental phase transition-sensitive band at 60 cm^{-1}. The problem of spectral attribution is significant both in the experiment and in theory because numerous atoms in an elementary cell generate series of experimental bands and calculated modes; an even more complicated case is that many of these bands are still complicated and they are difficult to approximate by individual Lorenz curves. Thus, the combined approach to comparison of experimental and theoretical, polarized and nonpolarized spectra, as well as the correct choice of ratiometric equations, can provide mutual verification of the data, correct attribution of bands, and identification of specific directions in crystals and films based on them. The knowledge about pore orientation is used for implementation of many practically important anisotropic properties such as optical and mechanical applications requiring the optimum orientation of crystals or films.

FUNDING

This work was supported by the Russian Foundation for Basic Research (Russian Center of Scientific Information), project no. 21-52-12018.

ACKNOWLEDGMENTS

We are grateful to Dr. Irena Senkovska for the presented DUT-8 (Ni, Co) samples. The experiments were performed in the Common Use Center of the Krasnoyarsk Scientific Center, Siberian Branch, Russian Academy of Sciences.

CONFLICT OF INTEREST

The authors of this work declare that they have no conflicts of interest.

REFERENCES

1. J. Kim, J.-U. Lee, and H. Cheong, "Polarized Raman spectroscopy for studying two-dimensional materials," J. Phys.: Condens. Matter **32**, 343001 (2020). https://doi.org/10.1088/1361-648x/ab8848
2. B. Xu, N. Mao, Ya. Zhao, L. Tong, and J. Zhang, "Polarized Raman spectroscopy for determining crystallographic orientation of low-dimensional materials," J. Phys. Chem. Lett. **12**, 7442–7452 (2021). https://doi.org/10.1021/acs.jpclett.1c01889
3. M. A. Pimenta, G. C. Resende, H. B. Ribeiro, and B. R. Carvalho, "Polarized Raman spectroscopy in low-symmetry 2D materials: Angle-resolved experiments and complex number tensor elements," Phys. Chem. Chem. Phys. **23**, 27103–27123 (2021). https://doi.org/10.1039/d1cp03626b

4. Q. Song, X. Pan, H. Wang, K. Zhang, Q. Tan, P. Li, Yi. Wan, Yi. Wang, X. Xu, M. Lin, X. Wan, F. Song, and L. Dai, "The in-plane anisotropy of WTe2 investigated by angle-dependent and polarized Raman spectroscopy," Sci. Rep. **6**, 29254 (2016). https://doi.org/10.1038/srep29254
5. L. Svenningsson and L. Nordstierna, "Polarized Raman spectroscopy strategy for molecular orientation of polymeric fibers with Raman tensors deviating from the molecular frame," ACS Appl. Polym. Mater. **2**, 4809–4813 (2011). https://doi.org/10.1021/acsapm.0c00762
6. K. A. Okotrub, V. A. Zykova, S. V. Adishchev, and N. V. Surovtsev, "Determination of the orientation of phospholipid molecules in planar structures from Raman spectra," Optoelectron., Instrum. Data Process. **55**, 495–500 (2019). https://doi.org/10.3103/S8756699019050121
7. Ya. Wang, C. Cong, C. Qiu, and T. Yu, "Raman spectroscopy study of lattice vibration and crystallographic orientation of monolayer MoS_2 under uniaxial strain," Small **9**, 2857–2861 (2013). https://doi.org/10.1002/smll.201202876
8. Z. Li, R. J. Young, I. A. Kinloch, N. R. Wilson, A. J. Marsden, and A. P. A. Raju, "Quantitative determination of the spatial orientation of graphene by polarized Raman spectroscopy," Carbon **88**, 215–224 (2015). https://doi.org/10.1016/j.carbon.2015.02.072
9. G. S. Duesberg, I. Loa, M. Burghard, K. Syassen, and S. Roth, "Polarized Raman spectroscopy on isolated single-wall carbon nanotubes," Phys. Rev. Lett. **85**, 5436–5439 (2000). https://doi.org/10.1103/physrevlett.85.5436
10. J. Thyr, L. Österlund, and T. Edvinsson, "Polarized and non-polarized Raman spectroscopy of ZnO crystals: Method for determination of crystal growth and crystal plane orientation for nanomaterials," J. Raman Spectrosc. **52**, 1395–1405 (2021). https://doi.org/10.1002/jrs.6148
11. X. Liu, L. Zhang, and J. Wang, "Design strategies for MOF-derived porous functional materials: Preserving surfaces and nurturing pores," J. Materiomics **7**, 440–459 (2021). https://doi.org/10.1016/j.jmat.2020.10.008
12. M. Safaei, M. M. Foroughi, N. Ebrahimpoor, S. Jahani, A. Omidi, and M. Khatami, "A review on metal-organic frameworks: Synthesis and applications," TrAC Trends Anal. Chem. **118**, 401–425 (2019). https://doi.org/10.1016/j.trac.2019.06.007
13. Yi. Li and R. T. Yang, "Gas adsorption and storage in metal–organic framework MOF-177," Langmuir **23**, 12937–12944 (2007). https://doi.org/10.1021/la702466d
14. Q. Qian, P. A. Asinger, M. J. Lee, G. Han, K. Mizrahi Rodriguez, S. Lin, F. M. Benedetti, A. X. Wu, W. S. Chi, and Z. P. Smith, "MOF-based membranes for gas separations," Chem. Rev. **120**, 8161–8266 (2020). https://doi.org/10.1021/acs.chemrev.0c00119
15. Q. Wang and D. Astruc, "State of the art and prospects in metal–organic framework (MOF)-based and MOF-derived nanocatalysis," Chem. Rev. **120**, 1438–1511 (2019). https://doi.org/10.1021/acs.chemrev.9b00223
16. A. E. Baumann, D. A. Burns, B. Liu, and V. S. Thoi, "Metal-organic framework functionalization and design strategies for advanced electrochemical energy storage devices," Commun. Chem. **2**, 86 (2019). https://doi.org/10.1038/s42004-019-0184-6
17. H. D. Lawson, S. P. Walton, and C. Chan, "Metal–organic frameworks for drug delivery: A design perspective," ACS Appl. Mater. Interfaces **13**, 7004–7020 (2021). https://doi.org/10.1021/acsami.1c01089
18. A. Schneemann, V. Bon, I. I. Schwedler, I. Senkovska, S. Kaskel, and R. A. Fischer, "Flexible metal–organic frameworks," Chem. Soc. Rev. **43**, 6062–6096 (2014). https://doi.org/10.1039/c4cs00101j
19. Yu. Li, Yu. Wang, W. Fan, and D. Sun, "Flexible metal–organic frameworks for gas storage and separation," Dalton Trans. **51**, 4608–4618 (2022). https://doi.org/10.1039/d1dt03842g
20. S. Yuan, L. Zou, H. Li, Yi. Chen, J. Qin, Q. Zhang, W. Lu, M. B. Hall, and H. Zhou, "Flexible zirconium metal–organic frameworks as bioinspired switchable catalysts," Angew. Chem. **128**, 10934–10938 (2016). https://doi.org/10.1002/ange.201604313
21. V. Bon, N. Klein, I. Senkovska, A. Heerwig, J. Getzschmann, D. Wallacher, I. Zizak, M. Brzhezinskaya, U. Mueller, and S. Kaskel, "Exceptional adsorption-induced cluster and network deformation in the flexible metal–organic framework DUT-8(Ni) observed by in situ X-ray diffraction and EXAFS," Phys. Chem. Chem. Phys. **17**, 17471–17479 (2015). https://doi.org/10.1039/c5cp02180d
22. A. Krylov, A. Vtyurin, P. Petkov, I. Senkovska, M. Maliuta, V. Bon, T. Heine, S. Kaskel, and E. Slyusareva, "Raman spectroscopy studies of the terahertz vibrational modes of a DUT-8 (Ni) metal–organic framework," Phys. Chem. Chem. Phys. **19**, 32099–32104 (2017). https://doi.org/10.1039/c7cp06225g
23. L. Abylgazina, I. Senkovska, R. Engemann, S. Ehrling, T. E. Gorelik, N. Kavoosi, U. Kaiser, and S. Kaskel, "Impact of crystal size and morphology on switchability characteristics in pillared-layer metal-organic framework DUT-8(Ni)," Front. Chem. **9**, 293 (2021). https://doi.org/10.3389/fchem.2021.674566

24. S. Ehrling, I. Senkovska, A. Efimova, V. Bon, L. Abylgazina, P. Petkov, J. D. Evans, A. Gamal Attallah, M. T. Wharmby, M. Roslova, Z. Huang, H. Tanaka, A. Wagner, P. Schmidt, and S. Kaskel, "Temperature driven transformation of the flexible metal–organic framework DUT-8(Ni)," Chem.–A Eur. J. **28**, e202201281 (2022). https://doi.org/10.1002/chem.202201281
25. M. Mendt, F. Gutt, N. Kavoosi, V. Bon, I. Senkovska, S. Kaskel, and A. Pöppl, "EPR insights into switchable and rigid derivatives of the metal–organic framework DUT-8(Ni) by NO adsorption," J. Phys. Chem. C **120**, 14246–14259 (2016). https://doi.org/10.1021/acs.jpcc.6b04984
26. S. Ehrling, I. Senkovska, V. Bon, J. D. Evans, P. Petkov, Yu. Krupskaya, V. Kataev, T. Wulf, A. Krylov, A. Vtyurin, S. Krylova, S. Adichtchev, E. Slyusareva, M. S. Weiss, B. Büchner, T. Heine, and S. Kaskel, "Crystal size versus paddle wheel deformability: Selective gated adsorption transitions of the switchable metal–organic frameworks DUT-8(Co) and DUT-8(Ni)," J. Mater. Chem. A **7**, 21459–21475 (2019). https://doi.org/10.1039/c9ta06781g
27. A. Krylov, I. Yushina, E. Slyusareva, S. Krylova, A. Vtyurin, S. Kaskel, and I. Senkovska, "Structural phase transitions in flexible DUT-8(Ni) under high hydrostatic pressure," Phys. Chem. Chem. Phys. **24**, 3788–3798 (2022). https://doi.org/10.1039/d1cp05021d
28. H. Miura, V. Bon, I. Senkovska, S. Ehrling, N. Bönisch, G. Mäder, S. Grünzner, A. Khadiev, D. Novikov, K. Maity, A. Richter, and S. Kaskel, "Spatiotemporal design of the metal–organic framework DUT-8 (M)," Adv. Mater. **35**, 2207741 (2023). https://doi.org/10.1002/adma.202207741
29. Yi. Chang, S. He, M. Sun, A. Xiao, J. Zhao, L. Ma, and W. Qiu, "Angle-resolved intensity of in-axis/off-axis polarized micro-Raman spectroscopy for monocrystalline silicon," J. Spectrosc. **2021**, 2860007 (2021). https://doi.org/10.1155/2021/2860007
30. L. Nafie, P. Stein, B. Fanconi, and W. L. Peticolas, "Angular dependence of Raman scattering intensity," J. Chem. Phys. **52**, 1584–1588 (1970). https://doi.org/10.1063/1.1673171
31. Yu. Choi, K. Kim, S. Ye. Lim, J. Kim, J. M. Park, J. H. Kim, Z. Lee, and H. Cheong, "Complete determination of the crystallographic orientation of ReX_2 (X = S, Se) by polarized Raman spectroscopy," Nanoscale Horiz. **5**, 308–315 (2020). https://doi.org/10.1039/c9nh00487d
32. R. Dovesi, A. Erba, R. Orlando, C. M. Zicovich-Wilson, B. Civalleri, L. Maschio, M. Rérat, S. Casassa, J. Baima, S. Salustro, and B. Kirtman, "Quantum-mechanical condensed matter simulations with CRYSTAL," WIREs Comput. Mol. Sci. **8**, e1360 (2018). https://doi.org/10.1002/wcms.1360

Translated by A. Nikol'skii